CONF-970706--3

SAND97-1594C

Modeling an Optical Micromachine Probe

Anthony Mittas, Fred M. Dickey, Scott C. Holswade

Sandia National Laboratories
Albuquerque, NM, 87185-0328

Abstract

Silicon micromachines are fabricated using Surface Micro-Machining (SMM) techniques. Silicon micromachines include engines that consist of orthogonally oriented linear comb drive actuators mechanically connected to a rotating gear. These gears are as small as 50-μm in diameter and can be driven at rotation rates exceeding 300,000-rpm. Measuring and analyzing microengine performance is basic to micromachine development and system applications. Optical techniques offer the potential for measuring long term statistical performance data and transient responses needed to optimize designs and manufacturing techniques. We describe the modeling of an optical probe developed at Sandia National Laboratories. Experimental data will be compared with output from the model.

Key words: Micromachines, optical probe, performance analysis, optical modeling

1. INTRODUCTION

Micromachines are mechanical gears and actuator systems which are fabricated using Surface Micro-Machining (SMM) techniques. The process uses deposition of multiple polysilicon layers on a silicon substrate which when masked and etched properly generate a gear and linkage system mounted on the silicon wafer. In the same process comb-drive electrostatic actuators are fabricated on the wafer which are connected to the gear linkage. Two orthogonally oriented actuators are driven by properly phased electrical drive signals which in turn provide the rotational force necessary to turn the gear.[1] Diagrams of a micromachine gear, linkage, and actuator are shown in Figure 1. Micromachine development has introduced several sizes and shapes of gears, ranging from 50μm to 1mm diameter.

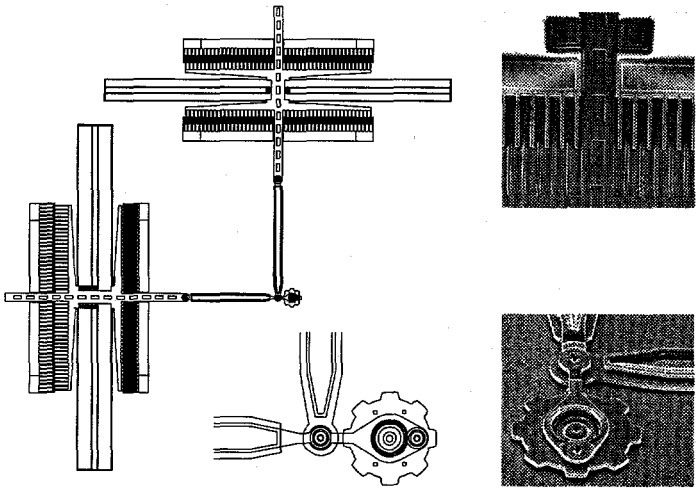

Figure 1. Micromachine gears, actuators, and comb drives.

The performance of MicroElectroMechanical systems, MEMS, must be monitored at all steps in the development process to analyze their response to variations in system design parameters and drive signals, and to identify fundamental degradation and failure mechanisms.[2] Presently, stroboscopic methods are used to characterize the rotation performance of MEMS gears. Stroboscopic methods incorporate high speed camera imaging to view the rotation of a gear

which shows an average effective rotation speed. In contrast, a single point optical probe using high bandwidth signal detectors will show a real time rotation rate. With a real time rotation rate, one can observe non-uniformity within one rotation of the gear which can not be seen with the stroboscopic methods.

In this paper, we discuss the modeling of the optical signals generated by an optical probe and how these signals can be used to analyze the performance of MEMS. The effects of probe spot size, spot position on the gear, and incident angle are examined as to how they effect the signals. The analysis of the signals can be used to determine rotation rate, rotation direction, uniformity of rotation rate, and gear position relative to the drive signals.

A model of the optical signals is useful in the design of future optical probes. This paper focuses on modeling of the forward and backscatter signal intensities reflected from a rotating gear. A 50μm diameter gear similar to that in Figure 2a is modeled. However, the size of the gear can easily be modified in the model to accommodate all the available sizes of gears such as the nineteen tooth gear in Figure 2b. The model simulates the available energy that is incident on the forward and backscatter collection optics and plots the power as a function of one gear rotation. The model accounts for the reflectance properties of the gear and substrate, the probe's spot size, the radial position of the probe's focal point, the incident angle of the beam, and the rotation direction of the gear.

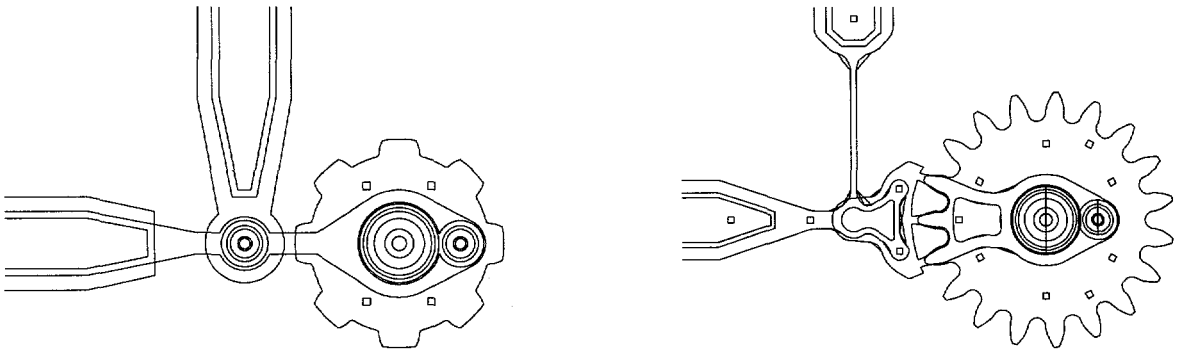

Figure 2. Micromachine gears. (a) eight tooth gear modeled and (b) nineteen tooth gear.

In the following section we discuss the probe performance requirements and design. Section 3 describes the model parameters and model function. In Section 4 we compare experimental waveforms from the optical probe with modeled optical signals and the work is summarized in Section 5.

2. MICROMACHINE OPTICAL PROBE

Rotation rate, angular speed, rotation direction, uniformity of rotation rate, and gear position relative to the drive signals (phase) are measurements required in the performance analysis of the MEMS gears. This information is also important as feedback in MEMS applications where gear position and rotation rate are required.[2] The current optical probe system is being developed to analyze the performance of MEMS gears and is shown schematically in Figure 3a. A photograph of the optical probe setup is shown in Figure 3b. The probe incorporates two detectors and one source. An unpolarized HeNe laser source is focused into a fiber and the output is collimated using lenses L1 and L2. The focus of L2 is located on the MEMS sample. The backscattered light is collected with L2 and collimated to the beam splitter, BS. L3 focuses the backscattered energy on the backscatter fiber which is connected to the backscatter signal detector. The forward scatter light is captured with a large diameter fiber which is connected to the forward scatter detector.

The forward and backscatter signals are dependent on the physical geometry and the reflectance properties of the gear and substrate surfaces. The backscatter signal is strongly dependent on the MEMS gear geometry. The backscatter signal amplitude is highest when the physical geometry of the gear and substrate act as a corner reflector and the incident light on the sample is reflected back toward L2.

The location of the peaks on the back scatter signal can be used to determine rotation rate of the gear. Either the forward or the backscatter signal can be used to observe the real time uniformity of motion not possible with the video

imaging stroboscopic method presently used. Comparing the phase relationship of the peak pulses between the forward and back-scatter signals can be used to determine the direction of rotation. The phase relation between these two signals is dependent on the location of the probe's focal spot relative to the surface of the gear.

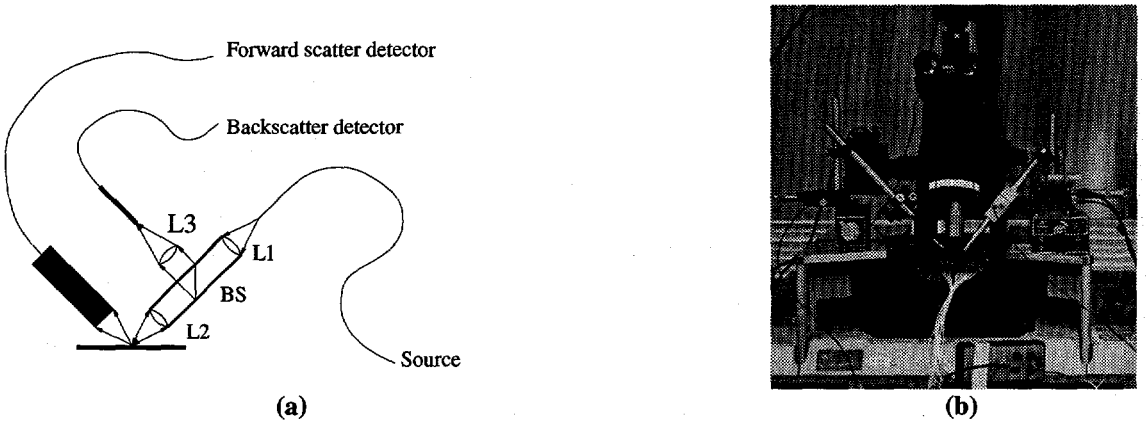

Figure 3. (a) Schematic diagram of the optical probe for forward and backscatter signal detection. (b) Photograph of the probe setup.

3. OPTICAL PROBE MODEL

The signals generated by the probe depend on the gear design parameters in a complicated way that is difficult to generalize. The model provides a tool by which the probe signals can be predicted and analyzed so that they may aid in the design of next-generation optical probes. The model uses the geometrical shape of the MEMS gear to create apertures for each reflecting surface of the gear. The intensity incident on the forward and backscatter planes from each reflective surface is calculated using the Fraunhofer (far field) approximation. The intensity on each plane is integrated to determine the incident power on the forward and backscatter planes. The incident power is plotted as a function of one gear rotation.

3.1. Gear Geometry

The shape of the gear teeth and their position relative to the substrate surface below them create the forward and backscatter signals in the optical probe. Figure 4 shows a side view of a gear tooth and the substrate illuminated by the incident beam from the optical probe. Two specular reflections are formed when the outside sections of the incident beam reflect off of the top of the gear and the substrate surfaces. The side surface of the gear tooth and the substrate surface form a corner reflector which creates two backscatter reflections of the incident beam from a substrate-to-gear and gear-to-substrate bounce of the incident light.

The incident beam from the optical probe is a tightly focused Gaussian profile beam with a calculated spot size $2\omega_0 = 1.83\mu m$, neglecting the lens aperture. The Rayleigh range is calculated at $z_0 = 4.16\mu m$. The top surface of the gear is nominally $4.54\mu m$ from the substrate surface under the gear. All the reflecting surfaces of the gear and substrate are within twice the Rayleigh range, $2z_0$, except at large incident angles to the sample plane. This allows the incident beam at the MEMS sample plane to be approximated by a plane wave.

The model simulates the intensity observed on the forward and backscatter planes from the probe's incident beam focused on the teeth of a rotating gear. The forward, backscatter, and sample planes are shown in Figure 5 along with the incident beam angle, θ_{inc}, and the specular reflected beam angle, θ_{ref}. The backscatter reflection angle is the same as the incident angle. The sample plane is the surface of the substrate under the gear and, for the figure only, includes the top surface of the gear. The difference in height between the gear's top surface and the substrate surface causes interference between the substrate and gear specular reflections at the forward scatter planes.

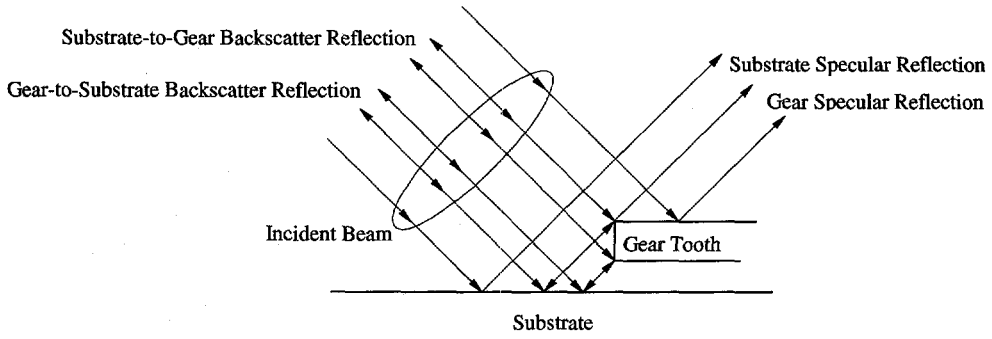

Figure 4. Forward and backscatter reflected beams created by the geometry of the gear teeth and the substrate below the gear from the incident optical probe beam.

Since the incident beam on each reflecting surface is approximated to be a plane wave, the forward and backscatter reflections originating at the MEMS sample plane can be approximated by apertures which are illuminated by the optical probe incident beam. The dimensions of the apertures are determined by the area of each reflecting surface exposed to the incident beam. The aperture area is dependent on the beam incident angle such that when the incident angle, θ_{inc}, is zero, the backscatter intensity becomes zero. The optical probe HeNe source beam is unpolarized so that bends in the source fiber and orientation of the source polarization do not change the polarization of the incident probe beam on the sample when the source fiber is repositioned. However, each of the reflected beams in Figure 4 are modeled as separate *s* and *p* polarized beams so that they can interfere with each other in the forward and backscatter planes. Each polarized reflected beam is translated to the forward and backscatter planes by a Fast Fourier Transform.

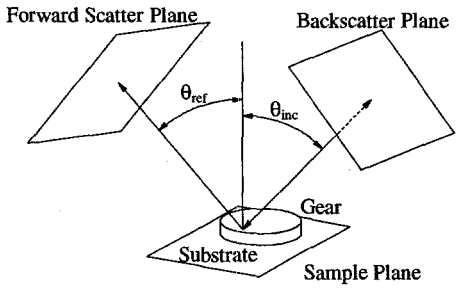

Figure 5. The three planes of interest used in the optical probe model: forward, backscatter, and sample planes.

3.2. Fraunhofer Diffraction

The criteria for using the Fraunhofer approximation is that

$$|\tilde{x}|, |\tilde{y}| << \sqrt{R_0 \lambda} \tag{1}$$

where $\tilde{x}$ and $\tilde{y}$ are half the aperture dimensions of a rectangular aperture back lit with a planar beam of wavelength λ and R_0 is approximately the aperture plane to image plane distance. Twice the Rayleigh range was determined to be $2z_0 = 8.32\mu m$ and all of the reflecting surfaces of a MEMS gear are within this range. Also, within twice the Rayleigh range, the focused beam can be approximated by a plane wave and the reflecting surfaces can be approximated by back lit apertures. In the case of a MEMS gear, the dimensions of a gear tooth side are 4.17μm and 2.54μm. The aperture to image plane distance is the distance from the sample plane to the lens, L2. For the optical probe, this distance is the focal length of L2, 8mm. Considering the largest tooth dimension, Eq. (1) becomes $2.09 < 71.2$ which is sufficient for this model. Calculations of intensity from a back lit aperture positioned at the beam waist and at the Rayleigh range are compared. The two calculations show no significant difference on the intensity observed on the image plane between the two positions of the aperture.

Figure 6 shows the projections of the reflecting surfaces from the gear and substrate onto the incident beam waist. Each projection on the beam waist is treated as a back lit aperture. The aperture for the gear and substrate reflections in Figure 6b and 6c can be simulated as half-plane apertures. The model then simulates the movement of the gear tooth passing under the incident beam. As the gear surfaces move through the beam, the aperture projections move along the beam waist in Figure 6 simulating the reflecting surfaces passing under the incident beam waist.

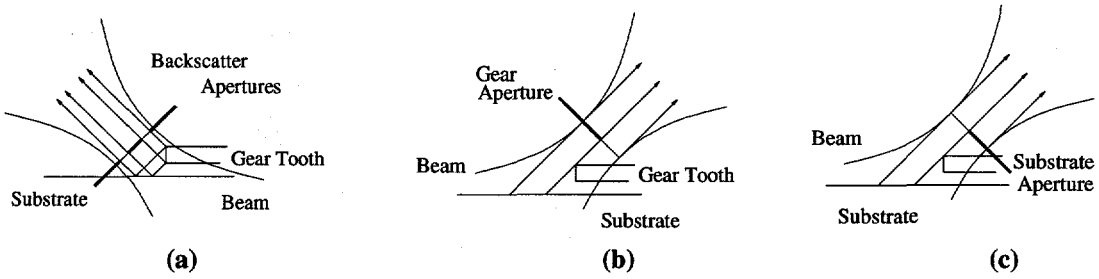

Figure 6. (a) Backscatter, (b) gear, and (c) substrate reflecting surfaces simulated as back lit apertures projected onto the incident beam waist.

3.3. Modeling Code

The model simulates the motion of a linear gear shown in Figure 7a. The gear teeth have the dimensions of the eight tooth, 50μm diameter gear in Figure 2a. The position of three gear teeth are modeled for a 45° turn of the gear relative to a stationary probe beam. Initially the beam is centered on the center gear tooth and the three teeth are moved so that the beam ends up centered on one of the other two gear teeth. Which tooth the beam ends up on depends on whether clockwise or counterclockwise rotation is simulated.

The motion of the gear during the 45° turn is divided into 101 positions of the three gear teeth relative to the incident beam. This number can be increased or decreased depending on the resolution required for the simulation. At each position, the incident beam is split up into its individual orthogonally polarized components reflecting from each surface of the gear and substrate. This is accomplished by multiplying the incident orthogonally polarized electric fields with transmission functions representing each of the reflecting surfaces on the sample plane.

A typical transmission function is shown in Figure 7b representing the top surface of the gear. The reflected intensity off of the gear at this position is shown in Figure 7c and a typical reflection off of the substrate is shown in Figure 7d. Note that the gear reflected intensity is viewed from a different orientation from the transmission function in Figure 7b so that the blocked part of the beam can be seen. Also note that the substrate reflection is shifted on the sample plane in the +y0 direction to account for the difference in height between the substrate and the gear top surface at the probe beam incident angle, 45° in this case. The difference in peak intensity between the intensity plots in Figure 7c and 7d are due to the different reflection properties of the gear and substrate at the 45° incident probe beam angle.

Each polarized electric field component is projected to the appropriate forward or backscatter plane (Figure 5) by a fast Fourier transform. At the forward and backscatter planes, the incident electric fields from each surface are combined and the intensity incident on each plane is calculated.

At each position of the three gear teeth, the power detected by the probe is calculated by integrating the intensity incident on the optical probe collection optics. The forward scatter plane collection optic is the 1mm diameter fiber and the backscatter plane collection optic is lens L2, with a diameter of 8mm. The calculated power at each position of the three gear teeth is plotted as a function of the 45° turn of the gear. This data is repeated for the number of teeth on a gear (eight in this case) and the simulated power collected at the forward and backscatter planes is plotted vs. the number of gear teeth positions in the simulation.

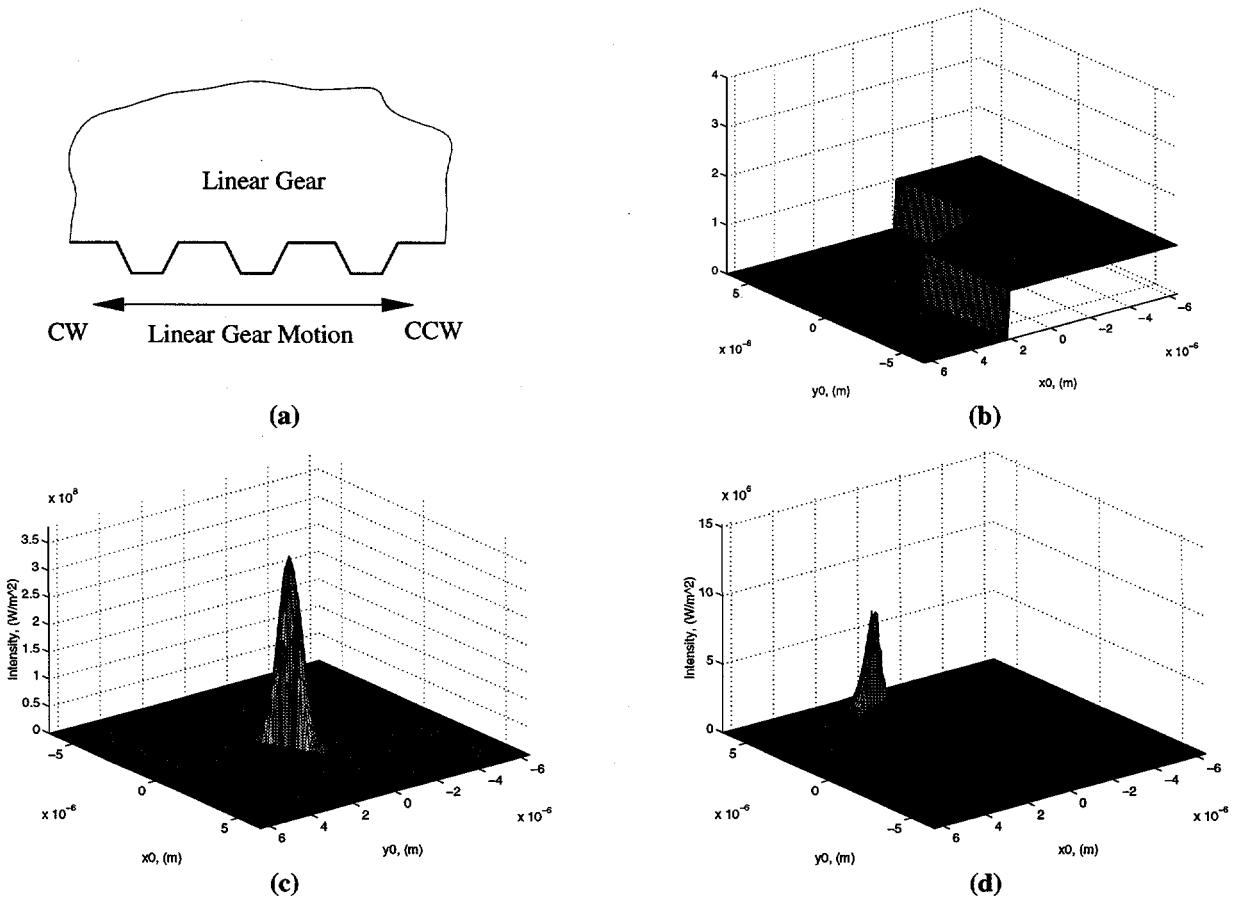

Figure 7. (a) Linear gear, (b) typical transmission function for top surface of linear gear, (c) intensity reflected from the gear surface, and (d) intensity reflected from the substrate surface.

4. EXPERIMENTAL RESULTS

This section describes the simulation capability of the model and compares simulated signals with experimental waveforms. The reflection properties of the gear and substrate surfaces are dependent on the layered structure of the MEMS machine and are used in the model to determine the reflected intensity from the gear and substrate surface. The reflection properties are determined experimentally and verified theoretically. They can be changed in the model to accommodate different layer material and thickness. This is discussed in Section 4.5.

The adjustable parameters of the model are: 1) gear rotation direction, 2) spot size, 3) radial position of the spot on the gear tooth, 4) beam incident angle, and 5) backscatter reflection angle. The gear rotation direction is either clockwise or counterclockwise from the top. The probe spot size is adjusted by defocusing the output end of the source fiber relative to the lens L1 in Figure 3. For most of the simulations, the beam is initially centered on a gear tooth. The radial position of the spot determines if the beam is located closer to the gear center or further away from the center. The backscatter reflection angle refers to the angle that the incident beam makes with the side of the gear tooth. The effect of this angle is to shift the backscatter intensity on the backscatter plane and is 0° for the simulations in this paper. Note that the amplitude scale for the simulation signals changes for each plot. This aspect is inherent in the model and allows for better resolution in the simulated signals.

4.1. Rotation direction

The simplest variable change in the model is the direction of rotation. The simulations in Figure 8a and 8b show probe signals for the gear turning counter clockwise and clockwise, respectively, when the gear is viewed from the top. Each figure shows the forward (top) and backscatter (bottom) signals generated for the two directions of rotation. The parameters for the two sets of data are 1.83μm spot size, the spot initially centered on the gear tooth, and 45° incident angle.

The backscatter signals shown in the bottom plots of Figure 8a and 8b exhibit two distinct peaks corresponding to the beam spot being incident on the gear-to-substrate and substrate-to-gear backscatter reflection apertures. As the beam spot passes between the two apertures the beam is incident on the air gap under the gear which corresponds to the beam being lost. The backscatter signal is zero when the beam is totally incident on the gear or substrate surfaces.

The peak in the forward scatter signal (top plots of Figure 8a and b) is representative of the beam being incident on the gear surface. The lower non-zero amplitude corresponds to the beam being incident on the substrate surface. The difference in amplitudes between these two parts of the signal is due to the reflection coefficients for the two surfaces at the 45° incident angle. The zero amplitude section of the signals correspond to the beam being reflected totally in the backscatter direction. The phase difference between the forward and backscatter signals in the clockwise rotation is opposite that in the counterclockwise direction. Signal processing the two sets of signals can extract the phase of each set of signals which can be used to determine the gear rotation direction.

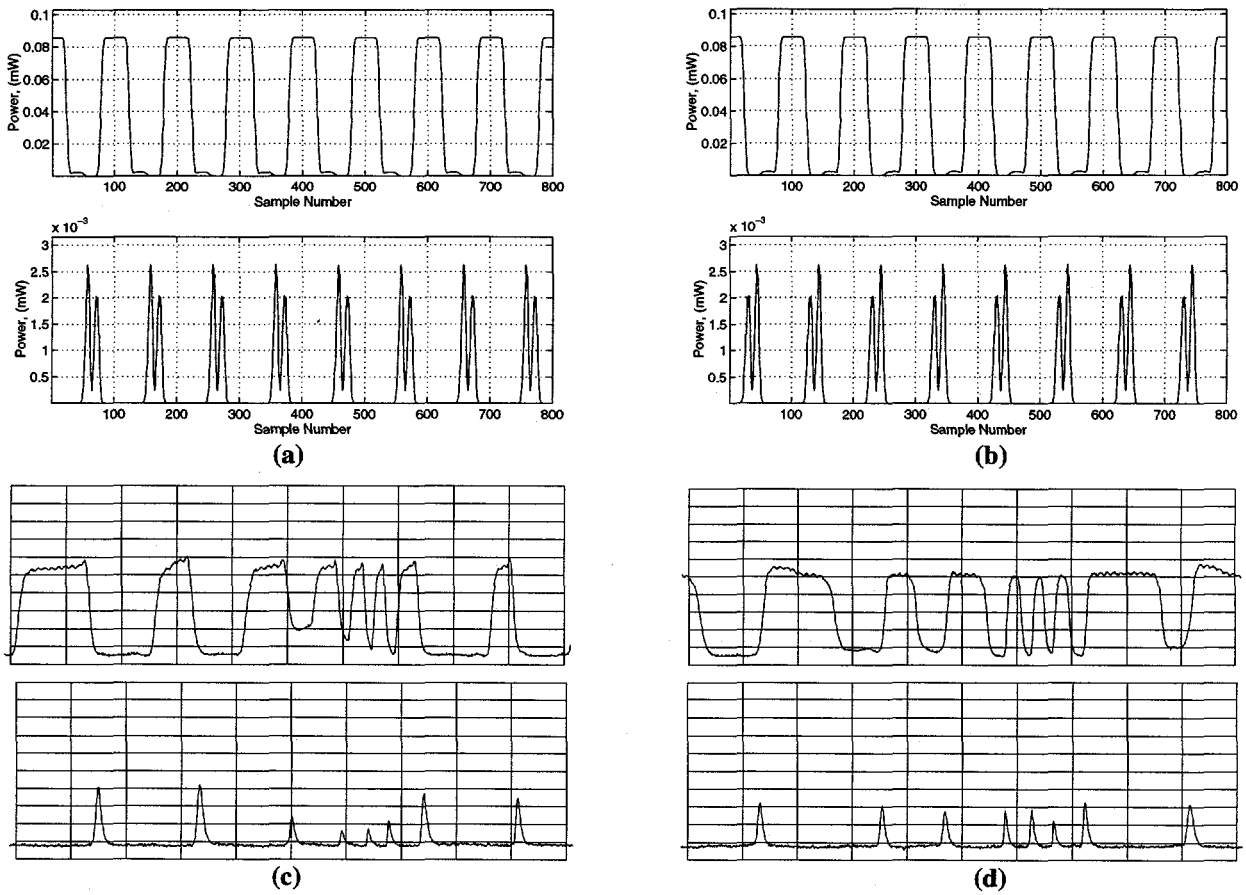

Figure 8. Simulation of the forward (top) and backscatter (bottom) signals of the gear rotating (a) counterclockwise and (b) clockwise from the top. Experimental forward (top) and backscatter (bottom) waveforms of the gear rotating (c) counterclockwise and (d) clockwise.

The waveforms in Figure 8c are experimental results captured on a digital signal analyzer of the forward and backscatter signals generated by the optical probe on a rotating gear. The gear is rotating at 500rps in the counter clockwise direction. The time scale is 200μs per division and the voltage scale is 100mV per division. Figure 8d shows the waveforms for the same gear rotating in the clockwise direction at 500rps. The time scale is 200μs per division and the voltage scale is 20mV per division. The incident angle of the probe beam is approximately 45°. The opposite phase relation is observed between the simulated signals and experimental waveforms. This is due to the different reflection properties between the sample tested for the model and the sample tested by the probe. However, one can use the phase relation between the forward and backscatter signals to determine rotation direction. Note the dip in the backscatter signals of Figure 8a and 8b and that the dip is not present in the backscatter waveforms of Figure 8c and d. The dip in the backscatter simulations is due to the probe beam being incident on the air gap between the gear and substrate. The reason that the dip does not show up in the experimental backscatter waveforms is that the optical probe detectors are bandwidth limited. This is discussed in Section 4.6. The non-uniform rotation rate shown in the waveforms is typical of MEMS performance at this time in their *development* because of non-optimized drive signals. The optical probe offers the ability to show this non-uniform rotation rate in a real time which is not available in the present stroboscopic analysis method.

4.2. Spot size

The probe spot size determines the resolution of gear teeth edges in the forward and backscatter signals as the gear rotates. The smaller the spot size, the faster the transitions are from one surface to the next. For an infinitely small spot, the transitions approach step functions. Figure 9 shows the forward and backscatter signals for four spot sizes ranging

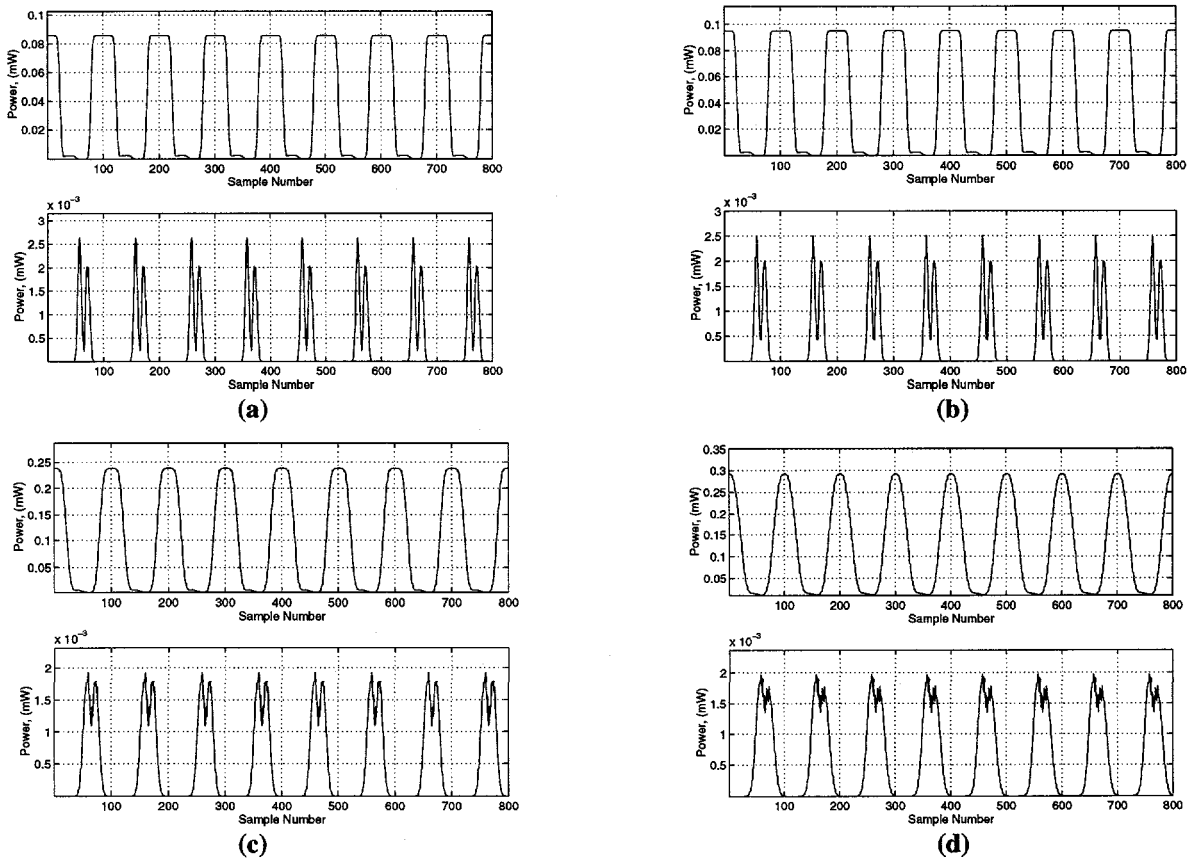

Figure 9. Forward (top) and backscatter (bottom) simulated signals as a function of spot size. (a) 1.83μm, (b) 2.00μm, (c) 4.00μm, and (d) 6.00μm.

from 1.83μm to 6.00μm. Each of the simulations is performed with the gear rotating counterclockwise, the spot initially centered on the gear tooth, and 45° incident angle. The figure shows that as the beam spot increases, the two peaks in the backscatter signal smooth out and the relative peak intensity decreases as each backscatter aperture collects less light.

The forward scatter peak amplitude changes as a function of the amount of beam incident on the gear surface. As the beam becomes larger, the beam begins to reflect from the inside of the gear hub which increases the amplitude in the forward scatter plane. Note that the forward scatter signal tends to round off as the beam spot increases and that the edge of the tooth is not as discernible with a large spot size.

4.3. Radial position

One aspect that needs to be considered is the tolerance required in positioning the optical probe spot on the gear for adequate forward and backscatter signals. In a manufacturing environment, the probe will be used to determine if MEMS gears fabricated on wafers are functioning. The simulations in this section can be used to analyze the forward and backscatter signal strength as a function of radial position on the gear and thus determine the required tolerance in positioning the probe. Figure 10a and 10b show forward and backscatter signals generated by the model as a function of the radial position of the probe spot. Both simulations are performed with the gear rotating counterclockwise, 1.83μm spot size, and 45° incident angle.

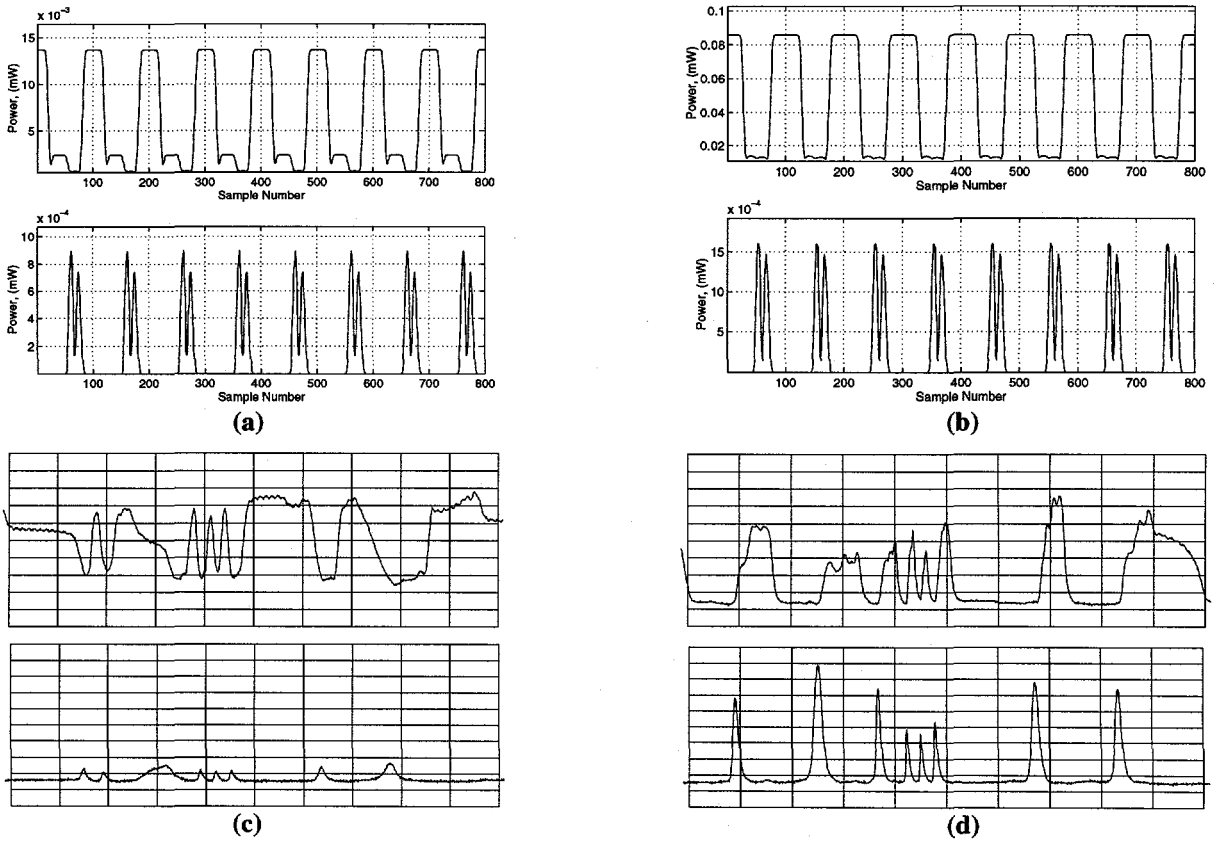

Figure 10. Forward and backscatter simulated signals for the beam located (a) on the outside edge of the gear teeth and (b) near the gear hub. Experimental forward and backscatter waveforms with the beam (c) on the outside edge of the gear teeth and (d) near the gear hub.

Figure 10c and 10d show forward and backscatter waveforms from the optical probe as a function of radial position on the gear tooth. Figure 10c represents the beam incident on the outside gear tooth edge and Figure 10d represents the beam incident on the inside gear hub. The time scale for the waveforms is 200μs per division and the voltage scale is

100mV per division for the forward scatter waveforms and 50mV per division for the backscatter waveforms. The gear rotation rate is 500rpm counter clockwise and the probe incident angle is approximately 45°.

The experimental forward scatter waveforms exhibit the opposite amplitude characteristics from the simulated forward scatter signals. This is due to the difference in reflection properties for the gear sample tested for the model and the gear under test with the optical probe. The model shows that the probe is tolerant of positional variations in the location of the probe focus and although the signal shape may change as a function of radial position, the gear rotation direction, speed, and speed variations are observable in real time.

4.4. Incident angle

Figure 11 shows the simulated forward and backscatter signals as a function of incident angle. The simulations are performed with the gear rotating counterclockwise, a 1.83μm spot size, and the beam spot initially centered on gear tooth.

The incident beam angle is equal to the specular reflected angle. For the simulations in this section, the reflected angle changes as the incident angle changes. This means that the physical location of the forward and backscatter planes change as a function of incident angle. At each location, the forward scatter plane is perpendicular to the specular beam and the backscatter plane is perpendicular to the incident beam.

The figure shows the variation in signal amplitude as a function of the beam incident angle. The amplitude variation as a function of incident angle is dependent on the reflection properties of the gear and substrate.

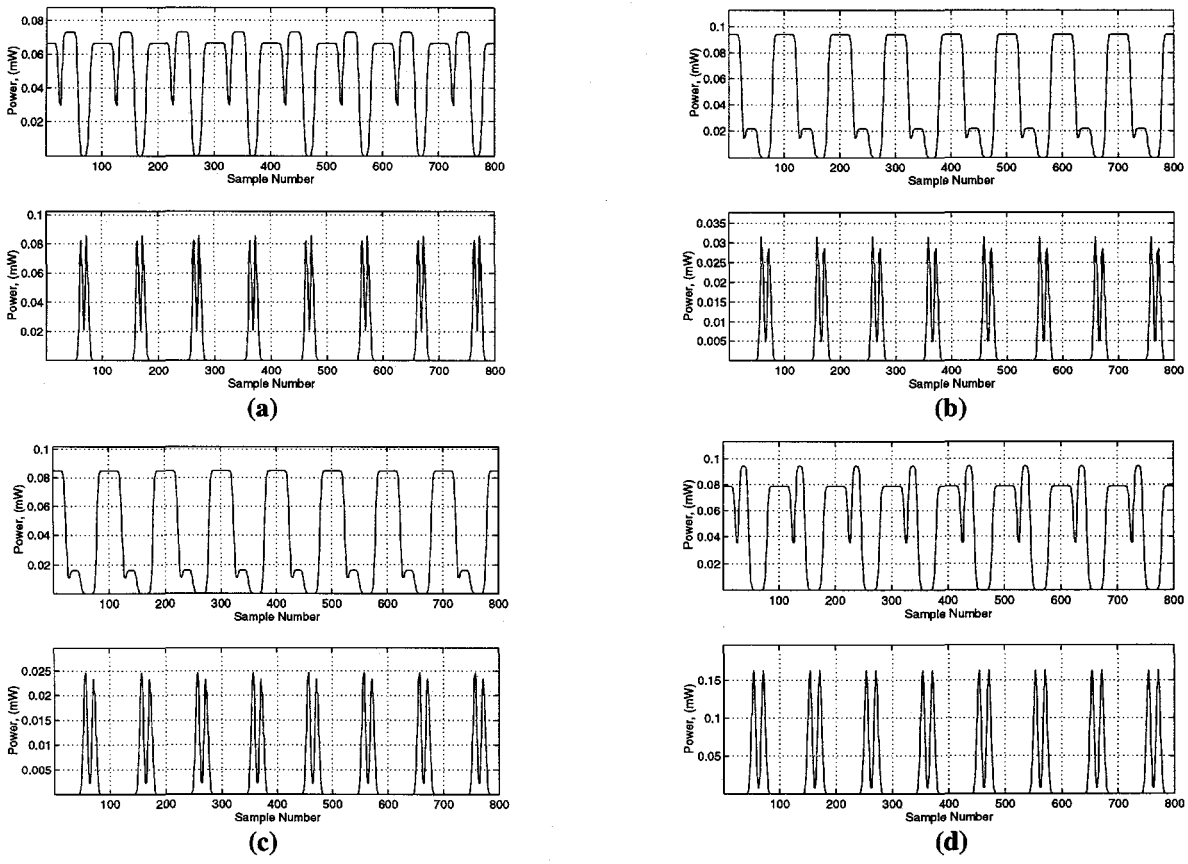

Figure 11. Forward and backscatter simulated signals as a function of incident angle. (a) 30°, (b) 40°, (c) 50°, and (d) 60°.

4.5. Material reflectance properties

In the design process of MEMS gears, different material layers may be introduced to improve the performance of the gears. The gear used to obtain the experimental waveforms in Sections 4.1and 4.3 is processed by a different method than the gear used to experimentally determine the reflectance properties of the gear and substrate used in the model. The model allows for changes to be made in the reflection properties of the surfaces so that other gear configurations can be modeled. The simulated signals in Figure 12 are used to compare the forward and backscatter signals when the reflection properties of the gear and substrate are reversed. The shape of the signals in Figure 12b more closely resemble the experimental waveforms in Figure 8c in that the reflectance from the substrate is higher than that of the gear. The simulated signals show that the gear rotation direction, speed, and speed variation are observable regardless of the reflection properties of the surfaces.

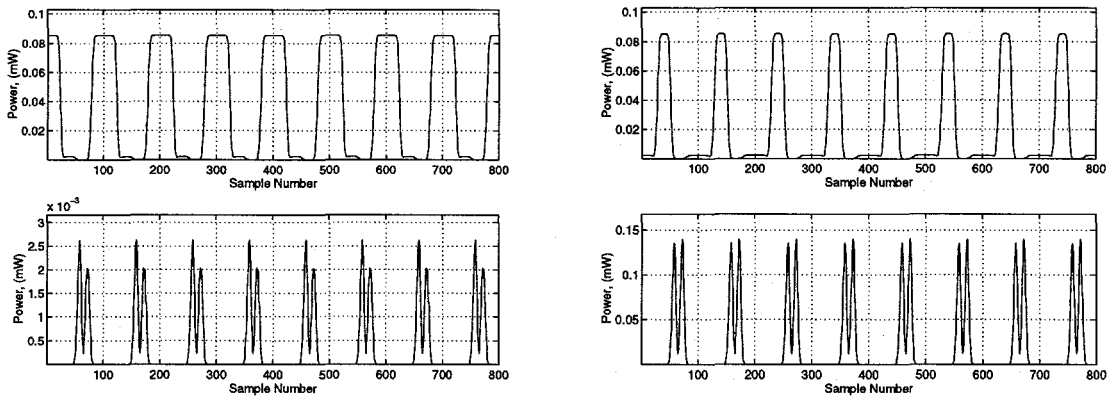

Figure 12. Forward and backscatter simulated signals for (a) experimentally measured gear and substrate reflectance properties and (b) reversed gear and substrate reflectance properties at a 45° incident angle.

4.6. Optical probe detector bandwidth

The rotation rate of the gears in Figure 8c and 8d and Figure 10c and 10d is 500rps and the gear teeth rate is 8 times (for eight teeth per gear) the rotation rate. This corresponds to a gear tooth frequency of 4kHz and a gear tooth period of 250μs. Consider the backscatter signal in Figure 8a with the gear rotating at 500rps. The backscatter pulse width (measured at the base) can be approximated to be 74μs. Within this pulse width there are four transitions, two rise times and two fall times. One of these transitions can be conservatively approximated to be the pulse width divided by four, or 19μs. The bandwidth associated with this rise time is calculated to be 18.4kHz.

The detectors used in the optical probe are New Focus Model 2001 which have adjustable upper and lower bandwidth settings and a built in signal amplifier. The maximum bandwidth is 300kHz and the maximum gain is 3×10^4. The backscatter waveforms in Figure 8c and 8d and Figure 10c and 10d are recorded at these detector settings. The detector amplifier –3db frequency at these settings is approximately 20kHz which corresponds to 22μs rise time. Comparing the detector bandwidth specified by the manufacturer, 20kHz, with the approximated 18.4kHz, one can see that the back scatter signal is at the limit of the detector amplifier bandwidth. It is possible that the two peaks observed in the backscatter simulated signals are not resolvable by the probe backscatter detector because of the detector amplifier bandwidth limit.

Further, FFT computations of the band limiting process confirms that the dip would not be resolved by the optical probe detectors. The forward scatter waveforms in Figure 8c and 8d and Figure 10c and 10d are also bandwidth limited by the optical probe detectors.

5. SUMMARY AND DISCUSSION

This paper describes a computer simulation model to predict the scattered signals from a micromachine optical probe when the probe beam is incident on a MEMS micromachine gear. The model uses measured and calculated reflection properties of the MEMS micromachine surfaces as well as the geometrical facets to model the scattered light into the forward and backscatter planes. The model calculates the power incident on the probe collection optics and plots the power as a function of gear rotation. The model provides insight into the dependence of the probe output on the optical properties of the gear, substrate, and probe geometry. From modeling the reflectance properties of the gear and substrate, the probe's spot size, the radial position of the probe's focal point, the reflected angle, and the incident angle of the beam, one can determine the optimum position for locating probe detectors. Knowing how these parameters effect the scattered optical signals, the probe design can be optimized for MEMS gear analysis or feedback in MEMS applications.

The simulations show that the model can predict the rotation direction of a gear based on the phase between the forward and backscatter signals. Comparing the simulated signals with the probe experimental waveforms shows that both sets of data exhibit different phase relationships for clockwise and counterclockwise rotation directions. The variation in spot size is shown to have no effect on the phase relationship of the forward and backscatter signals. However, the resolution of the gear teeth edges are a function of spot size. As the spot size increases, the transitions from one reflective surface to another are slower and the signal profile begins to approach a sinusoidal shape. The model has shown that the incident angle of the probe beam has no effect on the general shape of the backscatter signal over a range of 30° to 60°. The simulations show that the backscatter signal shape is narrower for low incident angles (and would be completely lost for 0° incident angle) because the backscatter apertures become narrower at these angles. For the most part, the beam shape is unchanged. This aspect implies that the backscatter signal may be more useful in determining the position of a gear tooth. The amplitude of both signals are affected as a function of the beam incident angle. This aspect can be exploited by future optical probe designs. For example, at different incident angles where the reflectance from the substrate in not at a minimum, the forward scatter signal becomes asymmetric. The shape of the forward scatter signal alone can be used to determine rotation direction.

The model demonstrated that the current design of the optical probe is adequate for determining gear rotation rate and direction. The model did not reveal any new aspects of the forward and backscatter signals that would suggest changes in the present optical probe design. The model did however reveal ranges for beam incident angles, beam spot size, and tolerances that can facilitate the development of future probes for specific measurement situations. The optical signals generated by the model can assist in the design of next generation versions of the optical probe. The simulated signals can be analyzed to determine the appropriate spot size and calculate the bandwidth requirements of the optical probe detectors. The model signals can generally apply to other gear geometries and other material reflection coefficients as the development of MEMS continue.

6. ACKNOWLEDGMENTS

The work for this paper was completed in fulfillment of a masters degree thesis at the University of New Mexico. The first author would like to thank Fred Dickey at Sandia and professor John McNeil at the university of New Mexico for co-chairing the thesis committee for which this work was performed. The authors would like to thank the assistance of Chris Raymond and John McNeil for the theoretical calculation of the gear and substrate reflection coefficients. Sandia is a multiprogram laboratory operated by Sandia Corporation, a Lockheed Martin Company, for the United States Department of Energy under Contract DE-AC04-94AL85000.

7. REFERENCES

1. J. J. Sniegowski and E. J. Garcia, "Microfabricated Actuators and Their Application to Optics", *Proceedings SPIE Miniaturized Systems with Micro-Optics and Micromechanics*, Vol. 2383. San Jose, CA, February 7-9, pp. 46-64, 1995.

2 F. M. Dickey, S. C. Holswade, N. F. Smith, S. L. Miller, "An Optical Probe For Micromachine Performance Analysis", *SPIE Proceedings*, Vol. 3008. San Jose, CA, February 10, 1997.

DISCLAIMER